



1857 FORT TEJON EARTHQUAKE: 150-YEAR RETROSPECTIVE

RMS SPECIAL REPORT



Risk Management Solutions

INTRODUCTION

On the morning of January 9, 1857, one of the largest earthquakes in California history occurred on the San Andreas Fault, rupturing over 300 km (186 mi) of the central and southern segments from near Parkfield at the northwestern end to San Bernardino at the southeastern end. Sometimes referred to as the Great California Earthquake of 1857, the event is most commonly known as the Fort Tejon Earthquake, as Fort Tejon was a military installation established by the United States Army in 1854, located near the center of the fault rupture and sustaining significant damage. According to historical accounts, the main shock occurred between 8:00 am and 9:00 am local time with felt effects as far away as Marysville to the north and San Diego to the south.

As there was little population in central and southern California in 1857, the estimated M_w 7.9 event resulted in only two reported deaths and destroyed a limited number of buildings. A repeat of this event in 2007, with its long period ground motions, has significant implications for the management of earthquake risk in California. Due to the population and property density in this region, substantial damage could occur. The 150th anniversary of the Fort Tejon Earthquake provides an opportunity to review historical accounts of the event, the potential impact of a repeat of the event and the implications of the earthquake 150 years ago on the seismicity of California today.



Figure 1: Southern California region showing length of 1857 fault rupture and extent of the felt region within California (north to Marysville and south to San Diego)

THE 1857 FORT TEJON EARTHQUAKE

What is known about the event of Friday, January 9, 1857 is largely based on historical accounts from those who felt the ground shaking. Newspaper accounts in the *Los Angeles Star*, the *Santa Barbara Gazette*, and the *San Francisco Daily Alta California*, among other newspapers, letters and memos at the time, were documented by Agnew and Sieh in 1978. These primary accounts, along with the surface rupture on the San Andreas Fault discernable in the years to follow, provide a way to estimate the extent of the felt region.

Most historical records agree that the ground shaking lasted from one to three minutes in the early hours of the morning – around 8:20 am PST. There is also agreement in the historical record that there were at least two strong foreshocks, the last being “about thirty minutes past six o’clock, A.M., on Friday, January 9” and two significant aftershocks on the evening of January 9 and a week later on the afternoon of January 16. Researchers continue to debate, however, on the epicenter location of this event. Based on the strong foreshocks occurring at the northern end of the fault rupture, the most likely epicenter location has been proposed at this end approximately 72 km (45 mi) northeast of San Luis Obispo and propagating to the southeast along the San Andreas Fault (Sieh, 1978b).

CHRONICLED DAMAGE

As there were scattered populations throughout the region in 1857, there were only two casualties reported: a woman at “Reed’s Rancho” near Fort Tejon and an elderly man near the Los Angeles area. This is consistent with the population density in southern California in the mid-19th century; according to the U.S. Census Bureau, in 1860 only three years after the earthquake, the population density was less than 3 people per square mile in the counties along the fault rupture (Figure 2). In 1860, the total population of the 15-county region analyzed as part of this report was 40,000 individuals.

Damage to buildings was also limited, with the most extensive damage reported at Fort Tejon. This military installation was established in 1854 to control the hostilities between the Native Americans and the white settlers at the time. A letter to the editor of the *Los Angeles Star* from the Quartermaster’s Deputy of Fort Tejon indicated that the earthquake shock resulted in “tearing the Officer’s quarters to pieces, severely damaging the Hospital, and laying flat with the ground the gable ends of nearly all the buildings erected, including the Quartermaster’s storehouse.” These observations were confirmed by a letter from Lieutenant Colonel B.L. Beall of Fort Tejon to his commanding officer saying that the “destruction to property, both public and private, has been immense.”

Along the fault rupture to the north and south of Fort Tejon, scattered damage was reported as “pieces of mortar fell from the walls” near San Benito and “private houses are also cracked, some of them very considerably” in Los Angeles. As far away as San Francisco, “in one instance a pile of merchandise in a store, in the lower part of Clay Street, was thrown to the ground.”

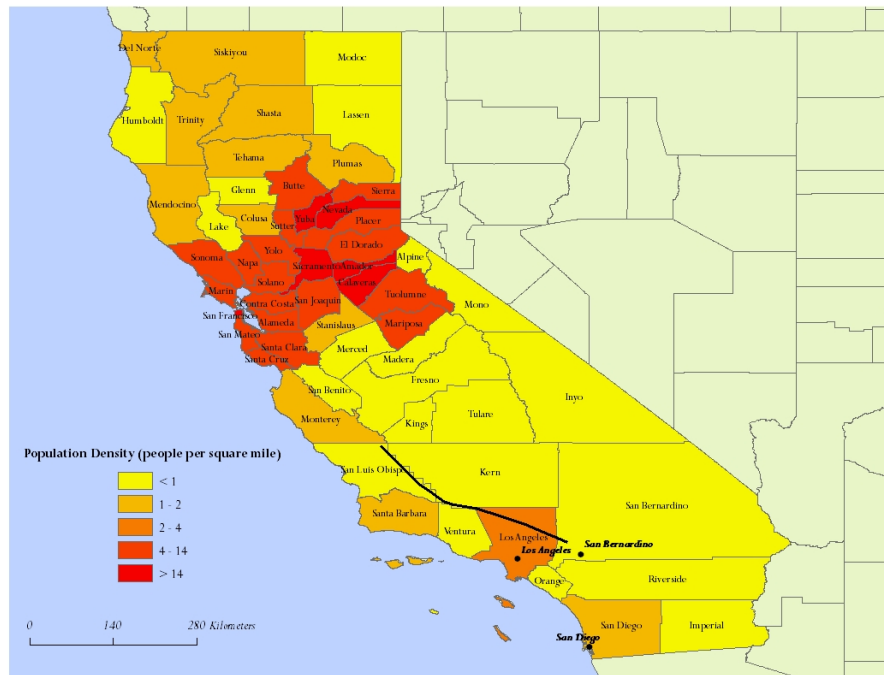


Figure 2: Concentration of California population in 1860 showing the majority of the population in northern California

GROUND MOTION AND LONG PERIOD EFFECTS

Despite the challenge of working with these historical records, researchers have managed to reconstruct intensity distributions for the 1857 event and constrain some of the source parameters. In particular, maps of Modified Mercalli Intensity (MMI) were developed and documented in more recent years (e.g., Figure 3). Maximum intensities of IX or more have been estimated along the fault rupture with a magnitude estimate of M_w 7.9 based on measurements of fault slip. Historical records indicate that “in the vicinity of Fort Tejon... the ground opened up in places for thirty or forty miles, and from ten to twenty feet wide.” Offset measurements along the fault (Sieh, 1978a) confirmed these observations with measurements ranging from 3 m (10 feet) to 9.5 m (31 feet) along the main 300 km (186 mi) rupture length.

Along with measurements of fault slip and ground motion intensity, the 1857 event has also been classified as one with long period ground motions as “the movement seemed to be comparatively slow, giving things time to recover after moving in one direction.” The reported oscillation of water (i.e., seiches) in surrounding rivers supports this notion of large ground motions, as observers “were astonished to see Kern river running upstream.” In addition, changes in the flow of wells in San Jose where “for a moment the water ceased to flow from the pipes and then gushed out in greater volume and with more power than usual” substantiate the long period ground motion effects of this historical event.

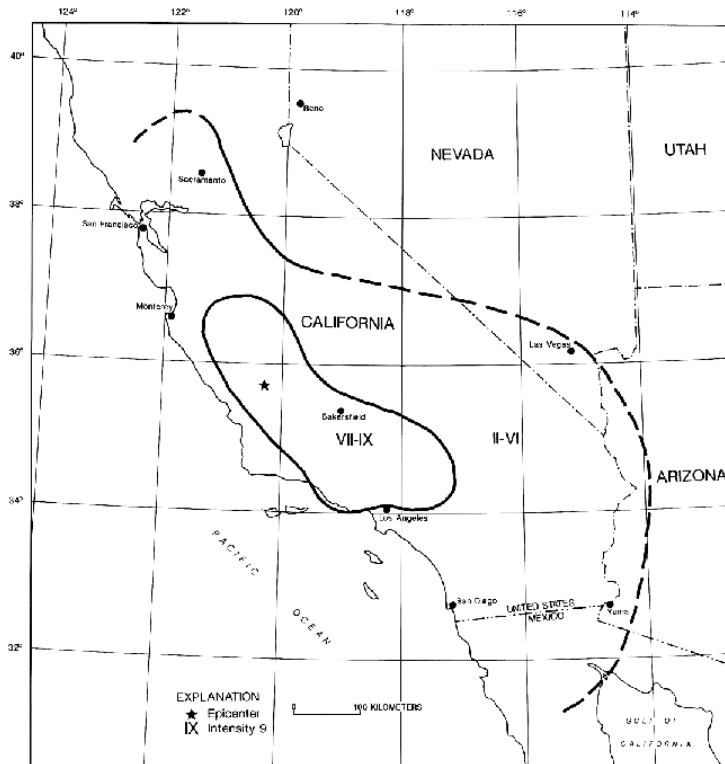


Figure 3: Isoseismal map of the 1857 Fort Tejon Earthquake (from Stover and Coffman, 1993)

THE FORT TEJON EARTHQUAKE IN 2007

For the 150th anniversary of the 1857 Fort Tejon Earthquake, RMS evaluated the potential impacts of an earthquake of a similar magnitude striking the central and southern California region in 2007. It should be noted that the earthquake modeled in this study is not the earthquake with the highest probability of occurring. The portion of the San Andreas Fault to the south of the rupture segment in 1857, from San Bernardino through the Coachella Valley to the Salton Sea, has not ruptured in over 300 years. According to the USGS, the next major earthquake in southern California is projected to occur on this section of the fault and cause major damage. In addition, there are hundreds of other faults throughout southern California which can be devastating to the region. The USGS-SCEC-California Geological Survey Working Group on California Earthquake Probabilities will release a new Uniform California Earthquake Rupture Forecast in 2007 incorporating substantial new scientific data. This consensus report will give the likelihood for a repeat of 1857, as well as probabilities for other significant anticipated earthquakes throughout southern California.

The Los Angeles metropolitan area comprises a very large area and is impacted by dozens of different seismic sources. Key strike-slip structures and thrust features in the Los Angeles area include the Newport-Inglewood, San Gabriel-Sierra Madre-Cucamonga, San Jacinto, Santa Monica, Palos Verdes and Puente Hills fault systems (Figure 4).



Figure 4: Map of southern California region showing fault systems with key faults and the 1857 rupture on the San Andreas Fault highlighted (in red)

HAZARD

This analysis assumed an M_W 7.9 earthquake on the central and southern segments of the San Andreas Fault, rupturing over 300 km (186 mi) of the strike-slip fault. The estimates of ground motion published by the USGS in ShakeMap format (Figure 5) were used to benchmark the results. However, as the next big earthquake on the San Andreas Fault will undoubtedly produce a unique ground motion pattern, a suite of attenuation models were utilized to estimate ground motion parameters (i.e., spectral acceleration).

In addition, the deep sedimentary basin underneath Los Angeles was modeled in this analysis, as the basin geometry and effects of deep soils provide a more complete representation of likely ground motion. However, the additional damage due to the liquefaction of unconsolidated soils is not significant as a result of this scenario event because areas of water-saturated sandy soil and artificial fill (e.g., along the coast) were not shaken very strongly (unlike in northern California where structures are built on artificial fills near the San Francisco Bay and very susceptible to liquefaction).

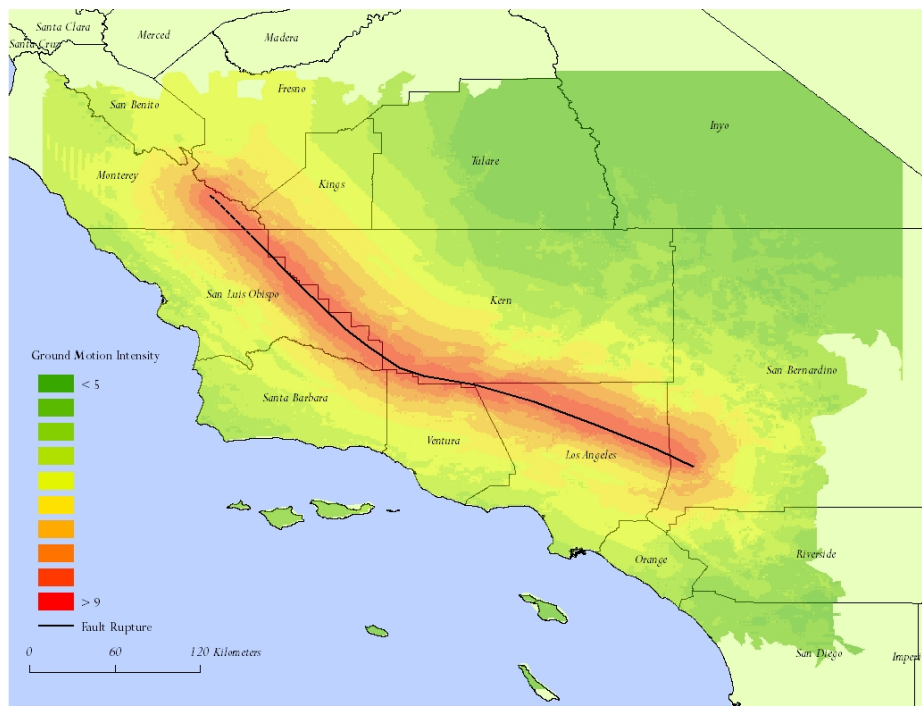


Figure 5: Modified Mercalli Intensity (MMI) from a repeat of the 1857 Fort Tejon Earthquake (based on the USGS MMI ShakeMap¹)

¹ USGS ShakeMap available electronically at http://earthquake.usgs.gov/eqcenter/shakemap/sc/shake/1857_se/ (December 2006)

EXPOSURE

In this scenario, ground shaking will impact fifteen central and southern California counties². According to the latest estimates from the U.S. Census Bureau, of the 23.9 million individuals living in the 15-county area, over 40% or close to 10 million people reside in Los Angeles County alone and 3.8 million reside in the city of Los Angeles. As a result, those individuals living north of the city but within Los Angeles County along the San Andreas Fault are particularly susceptible to this scenario event. Moreover, the region's working population is susceptible to injury while on the job and is dependent on the transportation networks within the region to move goods. As modeled here, the 1857 rupture cuts across several major interstates, including Interstate 5 which is the main north-south transportation route in the state.

RMS estimates the value of the building inventory in the fifteen analyzed counties, including structures and their contents, at \$350 billion for residential properties and \$380 billion for commercial and industrial properties (Figure 6). Of these estimates, approximately two-thirds of the value is attributed to property exposure and one-third to contents exposure. In addition, over 45% of the exposure value is in Los Angeles County alone. These inventory estimates are based on the 2006 RMS® U.S. Industry Exposure Database (IED), which captures exposures at the ZIP Code resolution for three primary insurance coverages: building/structure, contents, and time element (known as business interruption or additional living expenses). The U.S. IED incorporates policy details (limits and deductibles) for earthquake insurance in California in order that both economic and insured losses can be calculated.

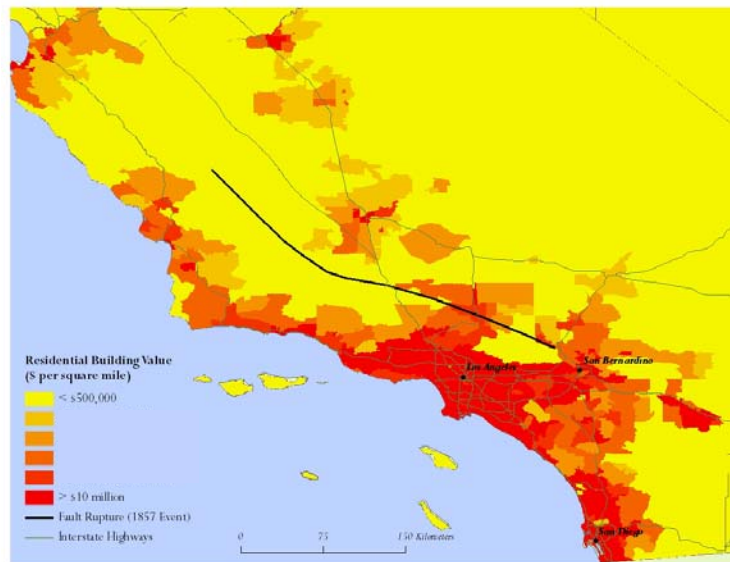


Figure 6(a): Building property exposure in the 15-county region, showing \$240 billion in residential building properties at risk

² The 15 counties are Fresno, Inyo, Kern, Kings, Los Angeles, Monterey, Orange, Riverside, San Benito, San Bernardino, San Diego, San Luis Obispo, Santa Barbara, Tulare, and Ventura

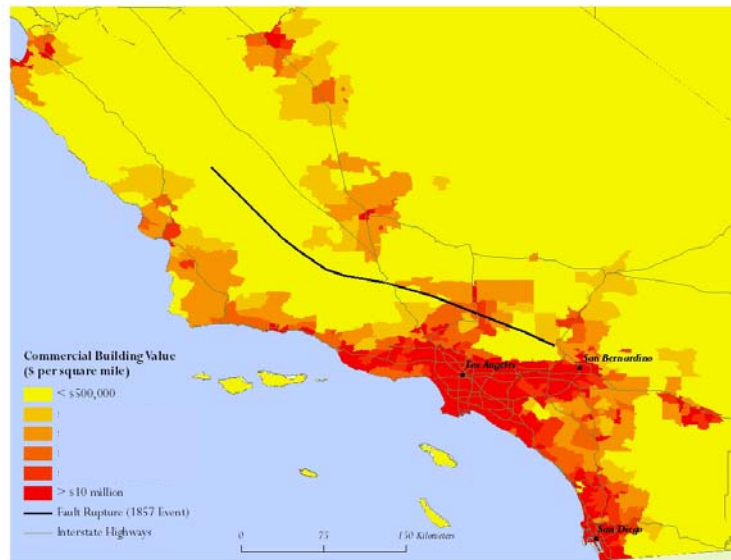


Figure 6(b): Building property exposure in the 15-county region, showing \$225 billion in commercial and industrial building properties at risk

BUILDING AND CONTENTS VULNERABILITY

The RMS spectral response methodology provides advance modeling of the vulnerability of property risks. The methodology uses an objective measure of ground motion intensity (spectral acceleration) to directly correlate ground motion to building performance based upon building height, construction material, and ground motion propagation. Individual vulnerability curves are used for predominant construction types in California (e.g., wood frame, reinforced concrete, reinforced masonry, steel frame) for buildings of various heights and years of construction.³ These individual vulnerability curves are important as different types of structures respond to the same earthquake ground motion in different ways. For example, an unreinforced masonry structure is more susceptible to damage than a reinforced concrete structure due to its ability to withstand the lateral load from the earthquake ground motion.

A building's height is an important driver of risk in this scenario event, as structures of various heights also respond differently to ground motions. Generally, low-rise structures (less than 3 stories) are stiff buildings damaged in earthquakes with 'high frequency' energy and tall structures (15 or more stories) are flexible buildings damaged in earthquakes with 'low frequency' energy. As this historical event contains 'low frequency' energy or long period ground motions, tall buildings at a distance from the fault rupture (i.e., in downtown Los Angeles) are more susceptible to damage.

³ For more information on damage susceptibility of California construction, see *The 1906 San Francisco Earthquake and Fire: Perspectives on a Modern Super Cat* (RMS, 2006).

Damage is also expected to contents, equipment, and inventories irrespective of any structural building damage. In the RMS approach to vulnerability modeling, contents damage assessment takes into account both ground shaking intensity and building performance. In the lower intensity events, contents damage is driven primarily by ground shaking; in higher intensity ground motion, both ground shaking and structural performance influence damage.

INSURANCE COVERAGES IN CALIFORNIA

In order for proper calculations of the percentage of monetary loss to be covered by insurance, an understanding of residential and commercial earthquake insurance coverage in California is necessary. For residential properties in California, earthquake insurance coverage can be purchased through a member insurer of the California Earthquake Authority (CEA) or a private insurer. In 2006, there were approximately 750,000 policies written by CEA insurers in the state of California. The basic CEA policy provided loss coverage for the residential structure but severely limits coverage for contents (\$5,000) and living expenses while the home is being repaired or rebuilt (\$1,500). All claims are subject to a 15% deductible. Private insurers compete within the marketplace as well, but only offer earthquake coverage as California law requires insurers to offer earthquake coverage as an endorsement to a homeowners policy. In this way, the private residential earthquake market can be more selective in the properties they cover and offer more comprehensive insurance (e.g., with lower deductible and higher limits than the basic CEA coverage).

In contrast to the residential earthquake insurance market, where the CEA statewide take-up rate is under 14%, the volume of commercial earthquake premium is several times that on residential exposure. Catastrophe models, such as the RMS[®] RiskLink U.S. Earthquake model, are used by commercial insurers to achieve technical risk-based returns while expanding levels of coverage to their commercial insureds. In 2007, the worldwide reinsurance market plays an essential role in this coverage.

ECONOMIC DAMAGE AND INSURED LOSS ESTIMATES

In the scenario outlined here, ground shaking would occur in all fifteen counties with the highest ground motions and subsequent damage ratios (defined as the ratio of the expected monetary damage to total exposed value) in the counties along the San Andreas Fault rupture, including San Bernardino, Kern, Los Angeles, San Luis Obispo and Ventura counties. Both economic damage and insured losses are calculated with the focus on insured losses. It should be reiterated that the losses are to the residential, commercial, and industrial properties in the region and insurance coverage includes loss to building/structure, contents, and costs due to displacement from a home or place of business (e.g., additional living expenses and business interruption).

Total economic damages are estimated at approximately \$150 billion with \$100 billion in residential damage and \$50 billion in commercial damage. The majority of this damage is due to ground shaking loss with a negligible percentage attributable to fire following the earthquake (< 0.01%). Combined insured losses from earthquake ground shaking are estimated to be between \$15 billion and \$25 billion for residential and commercial property coverages. While some damage would occur in all 15 counties, the three counties of San Bernardino, Los Angeles and Orange would sustain over 85% of the total insured loss (Figure 7).

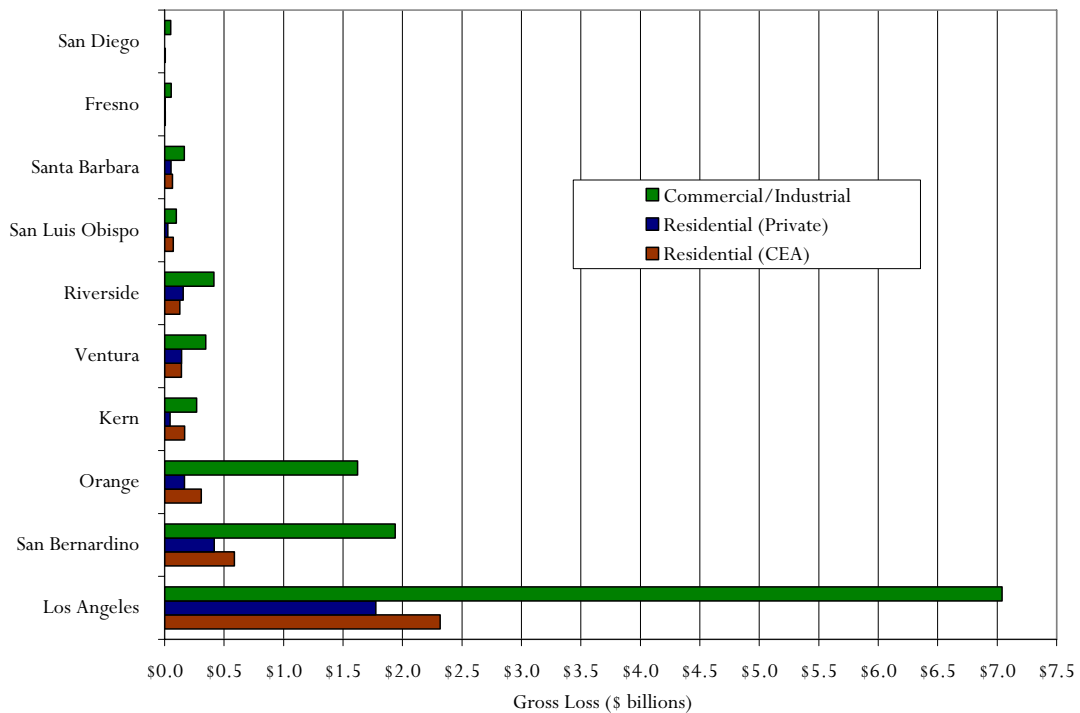
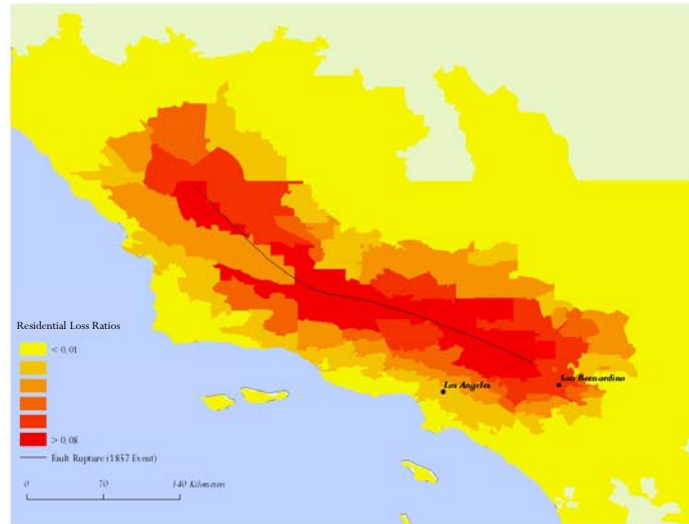
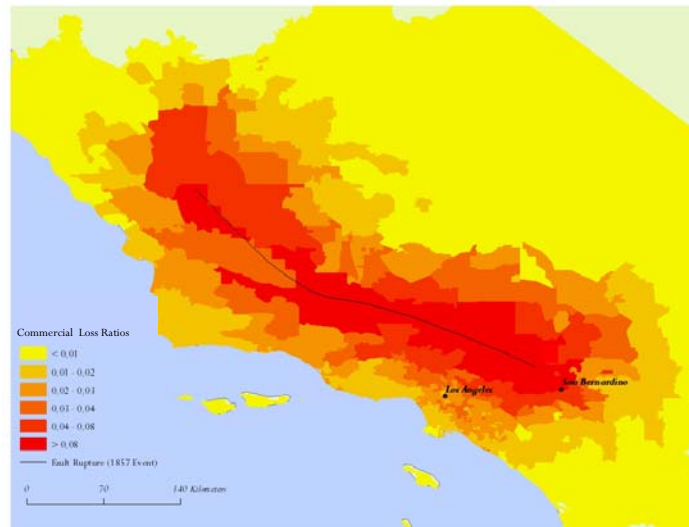


Figure 7: Estimated mean insured (gross) loss to the commercial and residential lines of business in the top ten of the 15 analyzed counties, showing the largest loss in Los Angeles County

The insured losses covered by the CEA and the private residential insurers are approximately one-third of this insured loss range (i.e., \$7 billion on average) with the other two-thirds covered by commercial insurers (i.e., \$13 billion on average). Unlike the 1994 Northridge Earthquake, where approximately one-third of the \$13 billion insured loss was to the commercial lines and two-thirds of the loss was borne by the residential insurance market, the significant majority of the losses expected in a repeat of the 1857 Fort Tejon Earthquake in 2007 would now be to commercial rather than personal lines. Moreover, due to the low take-up rate and limited coverage of the CEA policies, only slightly more than 6% of the expected \$100 billion in residential damages will be insured. Similarly, while the level of commercial coverage is substantially higher, 75% of the damage to commercial structures is not expected to be covered by insurance.



(a)



(b)

Figure 8: Average loss ratios, defined as the ratio of the net insured loss to the total limits, for ground shaking damage from a repeat of the 1857 Fort Tejon Earthquake to (a) the residential insurance market and (b) the commercial insurance market

COMPARISON TO THE 1906 SAN FRANCISCO EARTHQUAKE

In 2006, Risk Management Solutions went through a similar analysis to analyze the impact of a repeat of the 1906 San Francisco Earthquake in the Bay Area (see RMS, 2006). Nineteen counties in the northern California region were analyzed with \$1.2 trillion in residential exposure and \$750 billion in commercial exposure. Economic damages due to ground shaking and fire following earthquake totaled \$260 billion to the residential and commercial properties with the insured portion of this exposure, in combination with worker's compensation claims, would result in an insured loss between \$50 billion and \$80 billion.

In absolute terms, the overall economic and insured loss estimate from a repeat of the 1857 Fort Tejon Earthquake of about \$150 billion is significantly lower than for a repeat of the 1906 event. Additionally, the expected worker's compensation claims for the 1857 event is fairly inconsequential (i.e., this event is not considered a major casualty event). However, the ratio of economic damages to exposed value is higher for this event. Of the \$730 billion in exposure, \$150 billion is damaged in southern California (i.e., 20% damage ratio) in contrast to \$260 billion in damages to \$1.95 trillion in exposure in the San Francisco Bay Area (i.e., 13% damage ratio). As a result, the 1857 Fort Tejon Earthquake should be one of a set of historical events which should be considered in the management of earthquake risk in the state of California.

IMPLICATIONS FOR CALIFORNIA SEISMICITY

When an earthquake occurs, it releases the stress accumulated on a fault during its seismic cycle and changes the stress field in the surrounding area. The time until a future earthquake on one of the surrounding faults can be advanced or delayed, depending on if the fault is in a region of enhanced stress or decreased stress, respectively. This is the basis of stress transfer theory which has been developed over the past 15 years and is accepted by a majority of the scientific community.

Large earthquakes can permanently change the time of occurrence of future earthquakes on nearby faults and stress transfer calculations allow for the determination of comprehensive short-term recurrence probabilities that are both time- and space-dependent. Two very large earthquakes which have struck California in historic times, the 1857 Fort Tejon Earthquake (M_W 7.9) and the 1906 San Francisco Earthquake (M_W 7.9), are examples of large earthquakes that permanently changed the landscape of earthquake risk in the surrounding region. The occurrence of each event released stress built up over hundreds of years on the pertinent section of the San Andreas Fault, causing changes in stress accumulating on the surrounding faults and the subsequent estimates of timing of future fault ruptures.

This section explores the concept of stress transfer theory by first analyzing the changes in stress in the surrounding regions following the 1857 and 1906 earthquakes and then by examining the current accumulation of stress on the San Andreas Fault and its impact on California earthquake risk in 2007.

CHANGES IN STRESS DUE TO THE 1857 AND 1906 CALIFORNIA EARTHQUAKES

The 1857 and 1906 earthquakes were the largest earthquakes to have hit southern and northern California in historic times, respectively. Little is known about earthquakes in southern California prior to the 1857 event. However, historic mission and newspaper records in northern California indicate a high level of earthquake activity in the decades leading up to 1906 earthquake. In all, there were seventeen earthquakes of magnitude 6 or greater in the 70 years prior 1906 and only four since then (Figure 9). This marked drop in seismic activity is attributed to a ‘stress shadow,’ in which the stress was reduced on most faults in the Bay Area as a direct result of the 1906 San Francisco Earthquake.

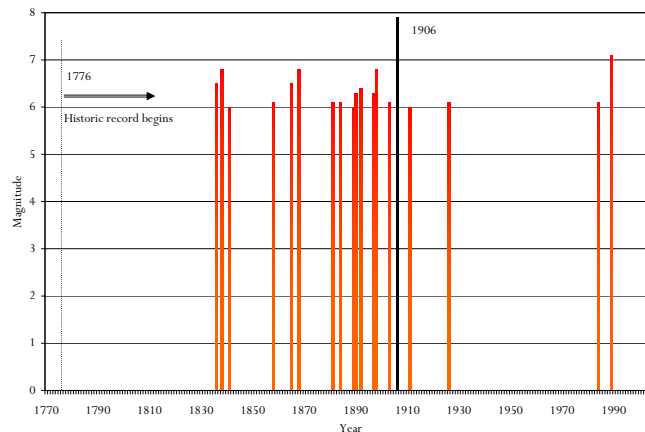


Figure 9: Seismicity of the Bay Area ($M \geq 6$) before and after the 1906 San Francisco Earthquake

It can be shown that regional stress changes resulting from both the 1857 and 1906 earthquakes significantly modified the occurrence time of subsequent events over hundreds of kilometers. Figure 10 shows the pattern of stress change caused by the 1906 earthquake. Areas of increased stress along all right-lateral faults of similar strike as the San Andreas Fault are represented in regions of orange and red and decreased stresses are in regions of blue and purple with the 1906 rupture represented in bold black. Regional seismicity represented by earthquakes of $M_W > 4.5$ during the 80 years following the 1906 earthquake is shown by black diamonds. As seen in the figure, the seismicity is concentrated primarily in regions of increased stress. Thus, the stress shadow created by this event explains the relative quiescence (i.e., lower seismicity rate) observed in the Bay Area since the beginning of the 20th century.

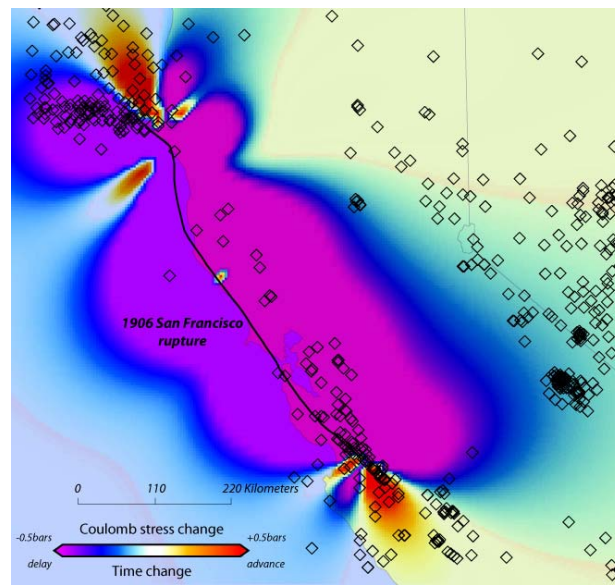


Figure 10: Stress changes due to the 1906 San Francisco Earthquake as changes impact strike-slip faults (Stress changes computed using slip distribution at depth determined from surveying data by Thatcher et al. (1997))

The earthquake history of southern California is also consistent with a similar stress shadow cast by the 1857 Fort Tejon Earthquake that substantially modified the time of occurrence of subsequent earthquakes during the 19th and early 20th centuries. Figure 11 shows stress transfer due to the 1857 earthquake in southern California. Because the stress changes on a nearby fault will depend of the characteristics of this fault (i.e., geometry and mechanism), the stress map presented in Figure 11(a) captures changes only to California strike-slip faults of similar strike (N145°).

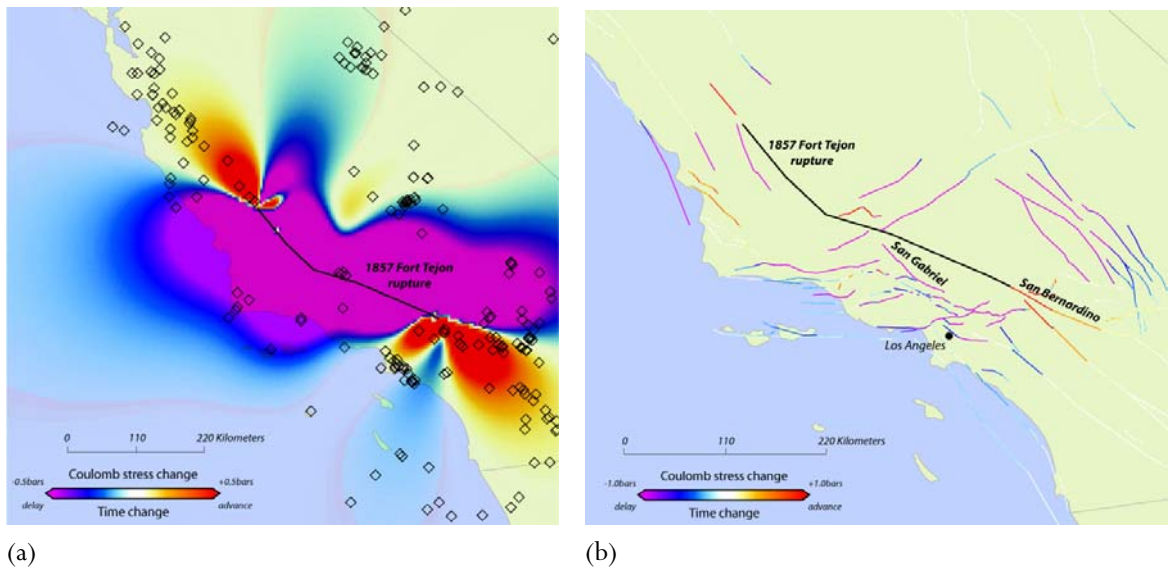


Figure 11: Stress changes due to the 1857 Fort Tejon Earthquake (a) as changes impact strike-slip faults and (b) as changes impact all active faults (Stress changes are determined using a smoothed version of Sieh's surface slip distribution (1978a))

In Figure 11(a), increased stresses are represented in orange and red colors and decreased stresses in blue and purple colors with the 1857 rupture represented in bold black. Harris and Simpson (1996) showed that the positive stress changes caused by the 1857 earthquake were consistent with the location of 13 of 15 moderate to large earthquakes ($M \geq 5.5$) that occurred in the 50 years after the event. They also concluded that 1857 earthquake delayed seismicity on faults that were relaxed by the earthquake for at least 50 years.

Historic earthquakes between 1857 and the installation of seismic recording instruments, as well as recorded seismicity of earthquakes with $M_w > 4.5$ until 1950, are shown as black diamonds. The majority of events are located in regions of increased stress (red regions) and very few events are located in the stress shadow (purple region). There are a few events observed in regions of decreased stress, which are not explained by stress transfer from the 1857 earthquake and can be explained by more complex models that determine the relative role of an earthquake on subsequent ones by simulating the stress field of each possible earthquake.

By taking into account the specific geometry and mechanism of each active fault from the RMS database, a fault-specific representation of stress changes is shown in Figure 11(b). In particular, the 1857 earthquake increased stress on both the San Jacinto and the San Bernardino segment of the San Andreas Fault, the latter of which has remained dormant for the past 300 years despite a long-term recurrence interval of about 150 years (Fialko, 2006).

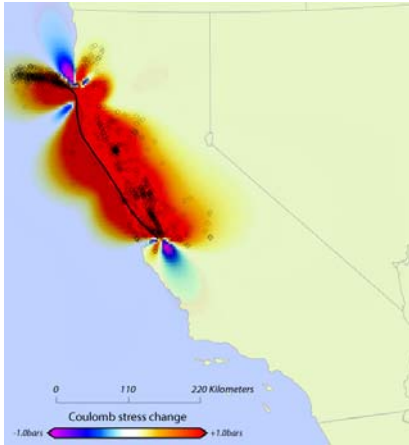
ACCELERATING SEISMICITY AND THE SAN ANDREAS FAULT

While these findings of changes in stress on the surrounding faults following the 1857 and 1906 earthquakes are important to understanding the probabilities associated with different magnitude earthquakes in the future, there is the potential of forecasting similar large events through the observation of increases in seismic activity in the region surrounding an impending event. This phenomenon, which is termed accelerating seismicity, is observed for years to tens of years before large earthquakes and has been considered for the past decade as a promising way to forecast large earthquakes. Accelerating seismicity has been observed systematically before large earthquakes where seismicity catalogs are of sufficient quality. It has already been identified in several active regions around the world (e.g., California, Greece, Japan, and New Zealand). However, to date no method exists to recognize this accelerating seismicity and utilize it to place a time frame for an impending event.

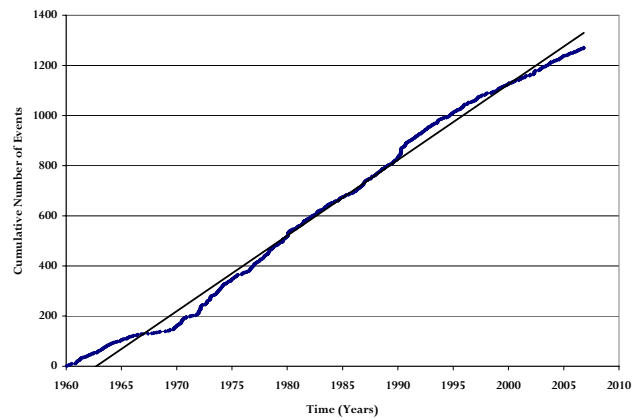
In the same way that the occurrence of aftershocks can be explained by stress transfer from the fault's rupture, it seems that accelerating seismicity can also be explained by stress transfer, but from accelerated loading on the fault which is going to rupture (King and Bowman, 2003). In that view, accelerating seismicity must occur in regions of increased stress due to an increased rate of loading. In theory, if regional seismicity located in regions of increased stress due to loading on a given fault presents an accelerating behavior, an earthquake can be expected in the next months or years on this fault. This approach has already been tested in a retrospective manner for the 2004 Sumatra Earthquake where a marked acceleration of seismicity began more than 20 years prior to the event (Mignan et al., 2006).

The historic records are too sparse and incomplete over time to test the accelerating seismicity hypothesis for the time period preceding the 1857 Fort Tejon and 1906 San Francisco earthquakes. Although the relatively high level of seismicity in the Bay Area in the decades prior to 1906 seems consistent, the earthquake records are not complete enough to establish accelerating seismicity. It is however possible to use this approach to determine if a new earthquake, equivalent to the 1857 or 1906 events in magnitude, is likely to occur in a near future somewhere along the San Andreas Fault. Following King and Bowman's stress accumulation model (2003), the evolution of seismicity through time since 1960 is determined in regions of increased stress due to loading on the San Andreas Fault.

Three regions are tested: the segment that ruptured in 1906 (Figure 12), the one that ruptured in 1857 (Figure 13) and the southernmost part of the San Andreas Fault (Figure 14). In Figures 12(a), 13(a), and 14(a), increased stresses are represented in orange and red colors and decreased stresses in purple and blue colors with the fault segments shown in bold black. Regional seismicity of $M_w > 3.5$ from 1960 to 2006 in regions of increased stress ($>1\text{bar}$) is represented by black diamonds. (Note that regions of increased stress and decreased stress are opposite of those in Figures 10 and 11, as the representation here is stress accumulation whereas in the earlier figures, it was stress release).

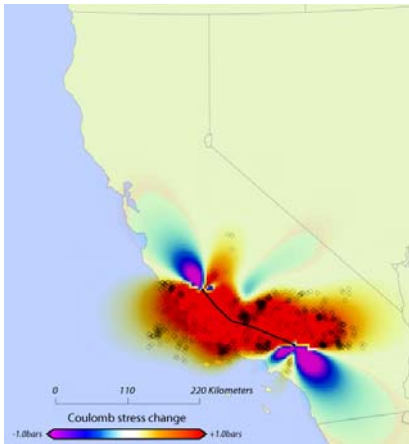


(a)

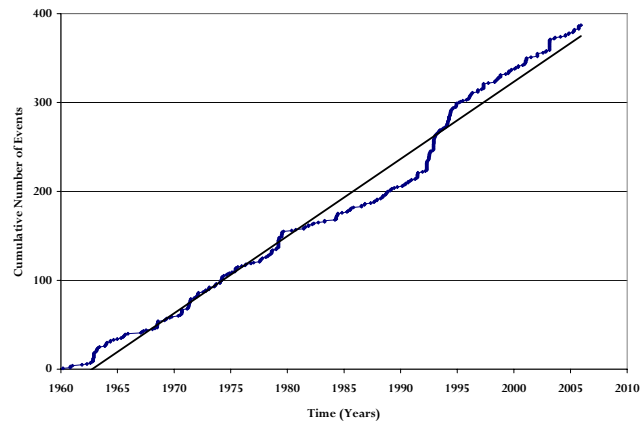


(b)

Figure 12: Accumulation of stress along the San Andreas Fault since 1960 along the 1906 San Francisco rupture (a) spatially and (b) through time (No accelerating seismicity is present, as shown by linear trend line)



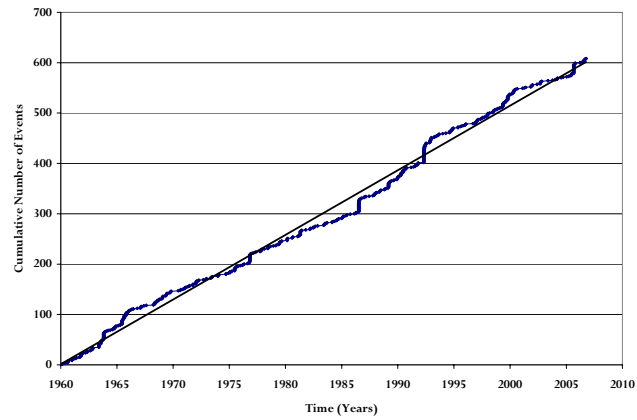
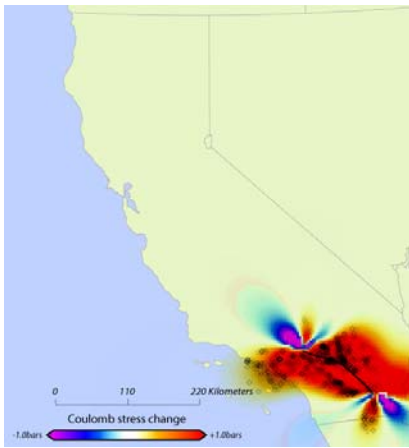
(a)



(b)

Figure 13: Accumulation of stress along the San Andreas Fault since 1960 along the 1857 Fort Tejon rupture (a) spatially and (b) through time (No accelerating seismicity is present, as shown by linear trend line)

From the representation of the seismicity evolution through time (defined here in terms of cumulative number of events) in regions of increased stress (Figures 12(b), 13(b), and 14(b)), preliminary tests show linear trends for all three regions. If accelerating seismicity were present, a concave upward trend would be seen. This indicates that the San Andreas Fault does have stress building but has not yet reached a critical level of failure and is unlikely to experience a major earthquake in the near future. However, the fact that no acceleration is observed does not necessarily mean that there is no acceleration, hidden by some seismic noise. For this reason, research on precursory seismicity continues apace to improve large earthquake forecasts.



(a) (b)

Figure 14: Accumulation of stress along the San Andreas Fault since 1960 along the southern part of the San Andreas Fault (a) spatially and (b) through time (No accelerating seismicity is present, as shown by linear trend line)

ACCELERATING SEISMICITY, STRESS TRANSFER AND RISK ANALYSIS

New models that integrate stress transfer and accelerating seismicity will lead to a better comprehension of the seismic risk in a given region, by refining probability calculations. By taking into account regional seismicity and the whole spectrum of physical parameters for each active fault in a region with all possible interactions, new probabilities can be determined that will improve seismic risk analysis by calculating the migration of the risk through time and space.

As leaders in our field, RMS remains committed to the continual research and implementation of improved approaches to modeling potential catastrophic losses. In developing more comprehensive models of earthquake risk, RMS will be working to ensure that emerging science such as accelerating seismicity is evaluated and considered for incorporation into future earthquake hazard models to assist our clients in making appropriate risk management decisions.

REFERENCES

- Agnew, D.C. and Sieh, K.E. (1978). A documentary study of the felt effects of the great California earthquake of 1857. *Bulletin of the Seismological Society of America*, 68 (6), p. 1717-1729.
- Fialko, Y. (2006). Interseismic strain accumulation and the earthquake potential on the southern San Andreas fault system, *Nature*, 441, p. 968-971.
- Harris, R. A. and Simpson, R. W. (1996). In the shadow of 1857 – the effect of the great Ft. Tejon earthquake on subsequent earthquakes in southern California. *Geophysical Research Letters*, 23, p. 229-232.
- King, G. C. P. and Bowman, D. (2003). The evolution of regional seismicity between large earthquakes. *Journal of Geophysical Research*, 108, p. 2096-2111.
- Mignan, A., King, G. C. P., Bowman, D., Lacassin, R., and Dmowska, R. (2006). Seismic activity in the Sumatra-Java region prior to the December 26, 2004 (Mw=9.0-9.3) and March 28, 2005 (Mw=8.7) earthquakes. *Earth and Planetary Science Letters*, 244, 639-654.
- Risk Management Solutions (RMS) (2006). *The 1906 San Francisco Earthquake and Fire: Perspectives on a Modern Super Cat*. http://www.rms.com/Publications/2006_SF_EQ_SuperCat.pdf
- Sieh, K. E. (1978a). Slip along the San Andreas fault associated with the great 1857 earthquake. *Bulletin of the Seismological Society of America*, 68, p. 1421-1448.
- Sieh, K. E. (1978b). Central California foreshocks of the great 1857 earthquake. *Bulletin of the Seismological Society of America*, 68, p. 1731-1749.
- Stover, C.W. and Coffman, J.L. (1993). *Seismicity of the United States, 1568-1989 (Revised)*. U.S. Geological Survey Professional Paper 1527, United States Government Printing Office, Washington.
- Thatcher, W., Marshall G., and Lisowski, M. (1997). Resolution of fault slip along the 470-km-long rupture of the great 1906 earthquake and its implications. *Journal of Geophysical Research*, 102, p. 5353-5367.